A Silica Nanochannel and Its Applications in Sensing and Molecular Transport

Bo Zhang,* Marissa Wood, and Hyunae Lee

Department of Chemistry, University of Washington, Seattle, Washington 98195-1700

We present the preparation, characterization, and analytical application of silica nanochannels in the size range of 5−100 nm. These cylindrical-shaped nanochannels are prepared using a simple laser-assisted mechanical pulling process, followed by partial enclosure into a glass micropipet. The nanochannels are characterized using a combination of optical microscopy, scanning electron microscopy (SEM), and resistance measurements in an electrolyte solution. The SEM results show that the nanochannel has circular geometry at the orifice. Ohmic response has been obtained from current−voltage measurements in KCl solutions using a silica nanochannel as small as 9 nm in diameter. These nanochannels have been utilized to sense single 40 nm polystyrene nanoparticles. A linear response has been observed between the detection rate and the concentration of nanoparticles in the range of 0−25 nM. The silica nanochannels have also been applied to the study of molecular transport of double-stranded DNA. Electroosmosis-driven molecular translocation has been observed for genomic-length λ-DNA through a 9 nm nanochannel in a 3 M KCl solution.

Nanometer-scale channels and nanopores have drawn enormous research attention in recent years due to their increasing application in a variety of fundamental and applied areas, such as separation of biomolecules,[1,2] detection[3−8] and manipulation[9−11] of single molecules, control of the molecular transport,[12−15] and fundamental investigation into the mass transport in geometrically confined spaces.[16−18] One of the most important properties of nanochannels is their large surface/volume ratio, which may lead to opportunities to study new physical phenomena previously inaccessible using large-scale devices.[18]

Successful applications of such nanofluidic devices often rely upon the preparation of structurally well-defined nanochannels. Many excellent technologies have been reported on the fabrication of nanochannels, each of which is usually most suitable for specific materials and geometries. A number of review papers have recently been published on this topic.[18−20] One of the most applied technologies is the wet/dry etching method used to obtain chip-based planar nanochannels.[21] A large aspect ratio is usually obtained between the width and the height of these channels. These channels are typically etched into glass, silicon, and silica using common clean room facilities. Another commonly used method is the so-called sacrificial technique, where a sacrificial layer is used as a template to generate the nanochannel.[22,23] Other outstanding techniques include nanoimprint lithography,[24] electron-beam[25,26] or ion-beam milling,[27] track-etching,[28] and a template method for constructing conical-shaped glass nanopores.[29,30]

We wish to report our recent research in constructing individual cylindrical-shaped silica nanochannels ranging from 5 to 100 nm in diameter. To fabricate these channels, a simple method based on laser-assisted mechanical pulling is developed

* To whom correspondence should be addressed. E-mail: zhang@chem.washington.edu. Phone: 206-543-1767. Fax: 206-685-8665.

(1) Han, J.; Craighead, H. G. *Science* **2000**, *288*, 1026–1029.
(2) Woods, L. A.; Gandhi, P. U.; Ewing, A. G. *Anal. Chem.* **2005**, *77*, 1819–1823.
(3) Gu, L. Q.; Braha, O.; Conlan, S.; Cheley, S.; Bayley, H. *Nature* **2000**, *398*, 686–690.
(4) Bayley, H.; Martin, C. R. *Chem. Rev.* **2000**, *100*, 2575–2594.
(5) Heins, E. A.; Siwy, Z. S.; Baker, L. A.; Martin, C. R. *Nano Lett.* **2005**, *5*, 1824–1829.
(6) Sexton, L. T.; Horne, L. P.; Sherrill, S. A.; Bishop, G. W.; Baker, L. A.; Martin, C. R. *J. Am. Chem. Soc.* **2007**, *129*, 13144–13152.
(7) Sun, L.; Crooks, R. M. *J. Am. Chem. Soc.* **2000**, *122*, 12340–12345.
(8) (a) Ito, T.; Sun, L.; Crooks, R. M. *Anal. Chem.* **2003**, *75*, 2399–2406. (b) Ito, T.; Sun, L.; Henriquez, R. R.; Crooks, R. M. *Acc. Chem. Res.* **2004**, *37*, 937–945.
(9) Tegenfeldt, J. O.; Prinz, C.; Cao, H.; Chou, S.; Rexisner, W. W.; Riehn, R.; Wang, Y. M.; Cox, E. C.; Sturm, J. C.; Silberzan, P.; Austin, R. H. *Proc. Natl. Acad. Sci. U.S.A.* **2004**, *101*, 10979–10983.
(10) Reccius, C. H.; Mannion, J. T.; Cross, J. D.; Craighead, H. G. *Phys. Rev. Lett.* **2005**, *95*, 268101.
(11) Reccius, C. H.; Stavis, S. M.; Mannion, J. T.; Walker, L. P.; Craighead, H. G. *Biophys. J.* **2008**, *95*, 273–286.
(12) Kemery, P. J.; Steehler, J. K.; Bohn, P. W. *Langmuir* **1998**, *14*, 2884–2889.
(13) Kuo, T. C.; Sloan, L. A.; Sweedler, J. V.; Bohn, P. W. *Langmuir* **2001**, *17*, 6298–6303.
(14) Wang, G. L.; Bohaty, A. K.; Zharov, I.; White, H. S. *J. Am. Chem. Soc.* **2007**, *129*, 7679–7686.
(15) Wang, G. L.; Zhang, B.; Wayment, J. R.; Harris, J. M.; White, H. S. *J. Am. Chem. Soc.* **2006**, *128*, 7679–7686.
(16) Powell, M. R.; Sullivan, M.; Vlassiouk, I.; Constantin, D.; Sudre, O.; Martens, C. C.; Eisenberg, R. S.; Siwy, Z. S. *Nat. Nanotechnol.* **2007**, *1*, 51–57.
(17) Kalman, E. B.; Vlassiouk, I.; Siwy, Z. S. *Adv. Mater.* **2008**, *20*, 293.
(18) Schoch, R. B.; Han, J. Y.; Renaud, P. *Rev. Mod. Phys.* **2008**, *80*, 839–883.
(19) Mijatovic, D.; Eijkel, J. C. T.; van den Berg, A. *Lab Chip* **2005**, *5*, 492–500.
(20) Abgrall, P.; Nguyen, N. T. *Anal. Chem.* **2008**, *80*, 2326–2341.
(21) Mao, P.; Han, J. Y. *Lab Chip* **2005**, *5*, 837–844.
(22) Gajar, S. A.; Geis, M. W. *J. Electrochem. Soc.* **1992**, *139*, 2833–2840.
(23) Stern, M. B.; Geis, M. W.; Curtin, J. E. *J. Vac. Sci. Technol., B* **1997**, *15*, 2887–2891.
(24) Liang, X. G.; Morton, K. J.; Austin, R. H.; Chou, S. Y. *Nano Lett.* **2007**, *7*, 3774–3780.
(25) Storm, A. J.; Chen, J. H.; Ling, X. S.; Zandbergen, H. W.; Dekker, C. *Nat. Mater.* **2003**, *2*, 537–540.
(26) Kim, M. J.; Wanunu, M.; Bell, D. C.; Meller, A. *Adv. Mater.* **2006**, *18*, 3149–3156.
(27) Li, J.; Stein, D.; McMullan, C.; Branton, D.; Aziz, M. J.; Golovchenko, J. A. *Nature* **2001**, *412*, 166–169.
(28) Siwy, Z.; Fulinski, A. *Phys. Rev. Lett.* **2002**, *89*, 198103.
(29) Zhang, B.; Zhang, Y. H.; White, H. S. *Anal. Chem.* **2004**, *76*, 6229–6238.
(30) Zhang, B.; Galusha, J.; Shiozawa, P. G.; Wang, G. L.; Bergren, A. J.; Jones, R. M.; White, R. J.; Ervin, E. N.; Cauley, C. C.; White, H. S. *Anal. Chem.* **2007**, *79*, 4778–4787.

10.1021/ac9009148 CCC: $40.75

to pull a silica microcapillary preform into a pair of ultrasharp tips. A short piece of the tip is then sealed into a glass micropipet to facilitate the measurement of the ionic current through the nanochannel. These nanochannels have been characterized using a combination of optical microscopy, scanning electron microscopy (SEM), and electrochemical voltammetry. The results show that the nanochannels have well-defined circular shape at the orifice and ohmic response in high-concentration KCl solutions. These nanochannels have also been utilized to sense polystyrene nanoparticles and to study the molecular transport of genomic-length double-stranded DNAs. We show that the electroosmotic flow could be strong enough to pull genomic-length DNA molecules through a sub-10 nm silica nanochannel. However, when the size of the nanochannel is increased, translocation of DNA is mainly driven by the electrophoretic force. To the best of the authors' knowledge, this is the first application of electroosmosis to stretch genomic-length DNA inside a sub-10 nm channel. Our results indicate that these silica nanochannels are geometrically well-defined and can be very useful in a number of different applications, such as the detection of single nanoparticles and the study of molecular transport through nanofluidic channels.

EXPERIMENTAL SECTION

Chemicals and Materials. KCl, KH_2PO_4, and K_2HPO_4 were all analytical grade bought from Aldrich and used without further purification. The 40 nm polystyrene (PS) nanoparticles with carboxylic functional groups were purchased from Bangs Laboratories, Inc. Quartz capillary tubing (o.d. = 1.0 mm, i.d. = 0.4 mm) was obtained from Sutter Instrument Company. Silica microcapillaries (o.d. = 0.35 mm, i.d. = 20 μm) were bought from Polymicro Inc. All aqueous solutions were prepared using >18.0 MΩ·cm water from a Barnstead Nanopure water purification system.

Preparation of the Silica Nanochannel. A laser-based micropipet puller (P-2000; Sutter Instrument Company) was used for the preparation of the silica nanochannels. The first step was to prepare a 1.0 mm silica preform containing a microchannel ~3−5 μm in diameter (e.g., ultrathick walls). To make such a preform, a 2 cm long silica microcapillary (i.d. = 20 μm, o.d. = 350 μm) was inserted into a 7.5 cm piece of 1 mm silica capillary tubing. One end of the tubing was closed with glue, and the ensemble was then mounted on a P-2000 laser micropipet puller. The other end of the silica tubing was connected to an in-house vacuum system through a piece of rubber tubing. With the two moving bars stabilized using a homemade aluminum clamp, the following heating program was then employed to seal the microcapillary into the 1 mm silica tubing: heat = 660, filament = 4, velocity = 100, delay = 100, pull = 1. The heating program was applied for 40 s followed by a 20 s cooling period. The above program was repeated until the size of the microchannel was reduced to ~3−5 μm. Three or four cycles were usually needed to obtain a complete seal and the right size of the microchannel preform.

In the second step, the vacuum and the clamp were removed from the puller and the following pulling program was executed to pull the preform into two ultrasharp silica nanotips: heat = 660, filament = 1, velocity = 60, delay = 165, pull = 225.

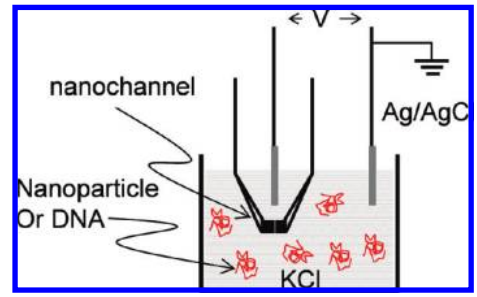

Figure 1. Schematic drawing of the electrochemical cell for measuring the translocation of polystyrene (PS) nanoparticles and DNA molecules through a single silica nanochannel.

Sealing a Silica Nanochannel in a Glass Micropipet Tip. To make a silica nanochannel, a short piece (usually between 5 and 100 μm) of the end portion of an ultrasharp silica nanotip was sealed into a glass holder made out of a borosilicate micropipet. A 2 mm borosilicate glass capillary and a P-97 glass micropipet puller were used to fabricate a micropipet holder. A silica nanochannel was carefully inserted into the end of a micropipet under an optical microscope. The end of the nanochannel was sealed into the borosilicate micropipet by quickly moving the micropipet tip through a natural gas flame. The nanochannel capillary was then pulled out of the borosilicate capillary, leaving a small portion of the nanochannel sealed together with the micropipet. The tip of the micropipet was then cut open with a sharp scalpel on an inverted cutting microscope.

Measurement of the Electrical Resistance. The current−voltage response was measured using a Chem-Clamp voltammeter−amperometer (Dagan, Inc.) as a potentiostat. The voltage signal was generated on a PAR 175 (Princeton Applied Research) universal function generator. The potentiostat was interfaced to a Dell computer through a PCI-6251 data acquisition board (National Instrument) via a BNC-2090 analog breakout accessory (National Instrument). The current−voltage data was recorded using in-house virtual instrumentation written in LabView (National Instrument). A one-compartment, two-electrode cell was employed with the cell and preamplifier in a home-built Faraday cage. Two Ag/AgCl wire quasi-reference electrodes are utilized for measuring the current−voltage response of the nanochannels.

Sensing of Single Nanoparticles and DNAs. A schematic drawing of the electrochemical cell for both nanoparticle sensing and the DNA translocations has been given in Figure 1. *All the voltages reported in the following text were applied on the Ag/AgCl electrode located inside the micropipet versus the one in the outside solution.* Nanoparticles and DNAs were added only to the outside solution, as shown in the Figure 1. An Axopatch 200B high-impedance amplifier (Molecular Devices, Inc.) was used for the sensing experiments. The current−time traces were acquired using a Digidata 1440a (Molecular Devices, Inc.) interfaced to a Dell computer. A 1.0 kHz low-pass filter on the 200B amplifier was used during the data acquisition. No further filtering was applied.

Microscopy. Optical images were acquired using a BX-51 microscope (Olympus) connected to a charge-coupled device (CCD) camera. SEM images were obtained using an FEI Sirion SEM. A 3 nm thick Au coating was sputtered on the silica nanochannels before SEM imaging. Transmission electron microscopy (TEM) images of SiO_2 nanochannels were acquired

on a Tecnai G2 F20 (FEI) microscope. No conductive coating was deposited on the silica nanochannel prior to TEM imaging.

RESULTS AND DISCUSSION

Nanochannel Fabrication. The construction of a silica nanochannel is inspired by the easy fabrication of glass micropipets using a commercial glass puller.[31,32] To obtain a cylindrical-shaped nanochannel by pulling, however, a silica capillary preform having a large o.d./i.d. ratio is preferred. Figure 2a shows an optical micrograph of such a capillary preform with a 1 mm o.d. and an ~3 μm i.d. (o.d./i.d ~ 330) after sealing a 20 μm silica capillary into a 1 mm silica capillary. The application of a negative pressure and the laser heating further decreases the size of the inner capillary after a seal is obtained between the two capillaries. The inset of Figure 2a displays an optical image of a typical silica capillary after being pulled on a laser puller. An arrow is added to indicate the location of the nanochannel. One can see that the inner capillary quickly decreases its size to below the resolution of the optical microscopy as the overall size of the capillary gets smaller. Figure 2b is an SEM image of a typical capillary tip. The tip is tilted to show the overall geometry of the ultrasharp tip. The length of the tip portion is usually measured to be from 1 to 2 cm depending on the parameters utilized in the pulling process. Therefore, the geometry of a thin piece (e.g., <100 μm) cut off the tip portion can be approximated by a cylinder. Figure 2c displays a high-resolution TEM image of the end portion of an ultrasmall silica nanochannel. The diameter of the inner channel is resolved to be ~5 nm.

To utilize the nanochannel for sensing and transport studies, a small piece (>5 μm in length) of the end portion of a silica tip is sealed into a borosilicate micropipet. Figure 2d shows an optical micrograph of a 10 μm long piece of a silica nanochannel after being sealed into a glass micropipet. To the left of the silica nanochannel is the tip of the nanocapillary from which the thin piece of the nanochannel is obtained. Silica nanochannels ranging from 5 to 100 nm can be easily prepared using this method. The size of the inner nanochannel can be determined using SEM and can also be computed from its ionic resistance, as described in the following section.

Characterization of the Silica Nanochannels. To fully describe the geometry of a cylindrical-shaped nanochannel, only two parameters are needed: the diameter, d, and the length, l. The length can be easily measured from an optical microscopic image for nanochannels longer than 5 μm. Both SEM and resistance measurements have been utilized to characterize the diameter of the silica nanochannel. Parts a and b of Figure 3 show SEM micrographs of a 130 nm silica nanochannel at low (Figure 3a) and high (Figure 3b) magnifications, respectively. The nanochannel orifice appears to be located in the center of the tip and is circular in shape. A smaller nanochannel is shown in Figure 3c, which is measured to be 38 nm in diameter. Due to charging effects at higher magnifications, we were unable to obtain satisfactory SEM images of even smaller nanochannels. However, the size of these smaller channels can be easily obtained from measuring their ionic resistance.

The ionic resistance of a cylindrical-shaped nanochannel can be expressed using the following equation:

$$R = \rho \frac{4l}{\pi d^2} \quad (1)$$

where R is the ionic resistance of the nanochannel, ρ is the resistivity of the electrolyte solution, and l and d are the length and the diameter of the nanochannel, respectively. Figure 4 shows current−voltage responses of silica nanochannels in a 10 mM

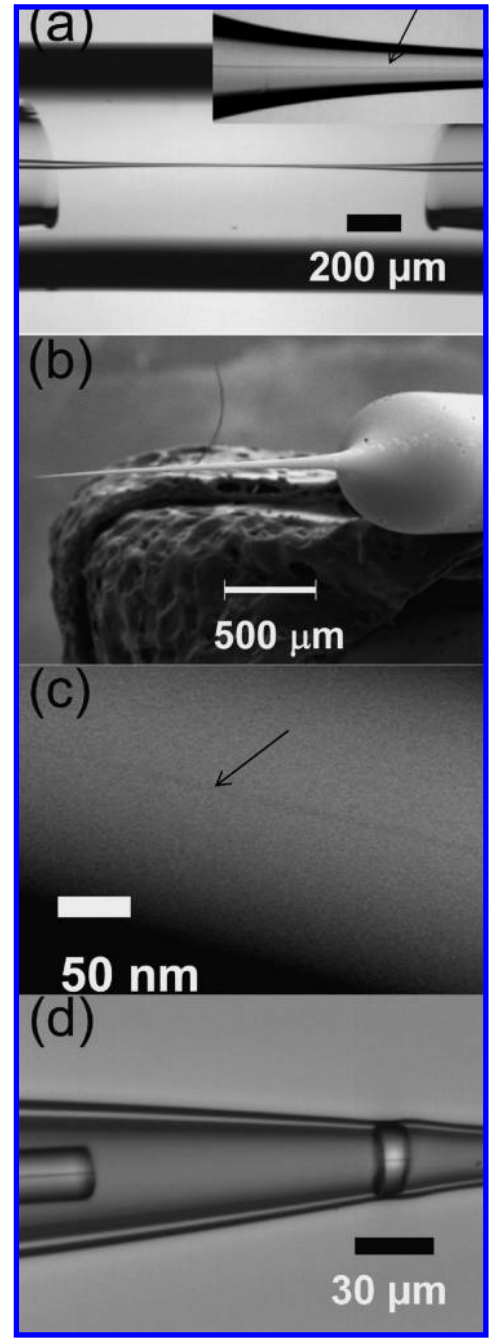

Figure 2. (a) Optical micrograph of a silica preform containing a silica microcapillary sealed in a 1 mm silica capillary; the inset displays an optical image of a typical silica capillary after being pulled on a laser puller. The arrow indicates the location of the nanochannel. (b) An SEM image of a silica capillary after being pulled. (c) A high-resolution TEM image of the tip portion of a pulled silica capillary containing a 5 nm channel. The arrow indicates the 5 nm nanochannel inside the thick silica. (d) An optical micrograph of a silica nanochannel sealed in a borosilicate glass micropipet.

(31) Munoz, J. L.; Coles, J. A. *J. Neurosci. Methods* **1987**, *22*, 57–64.
(32) Wei, C.; Bard, A. J.; Feldberg, S. W. *Anal. Chem.* **1997**, *69*, 4627–4633.

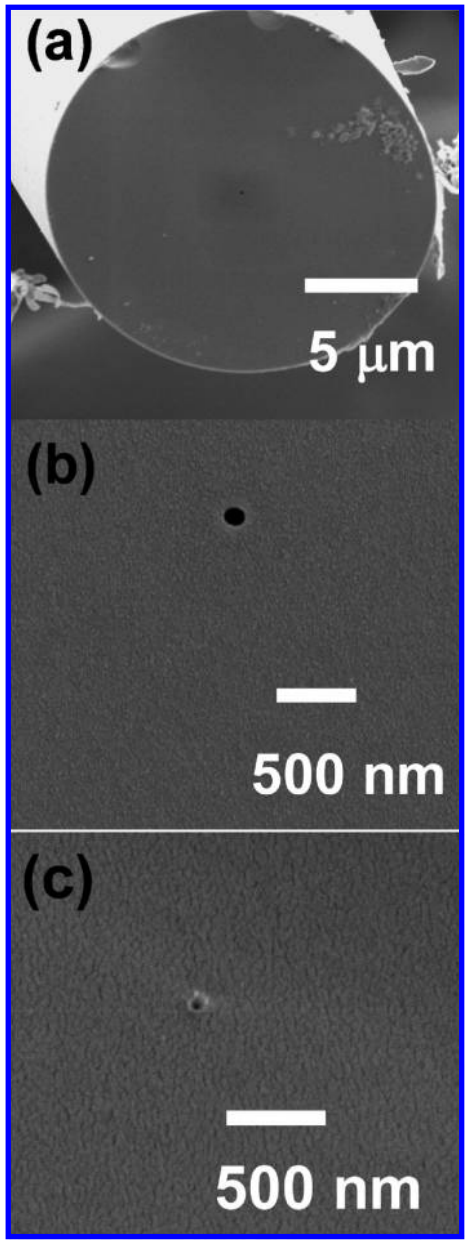

Figure 3. (a and b) SEM images of a 130 nm silica nanochannel: (a) a low-resolution image of the entire tip and (b) a high-resolution image of the circular opening. (c) A high-resolution SEM image of a 38 nm nanochannel.

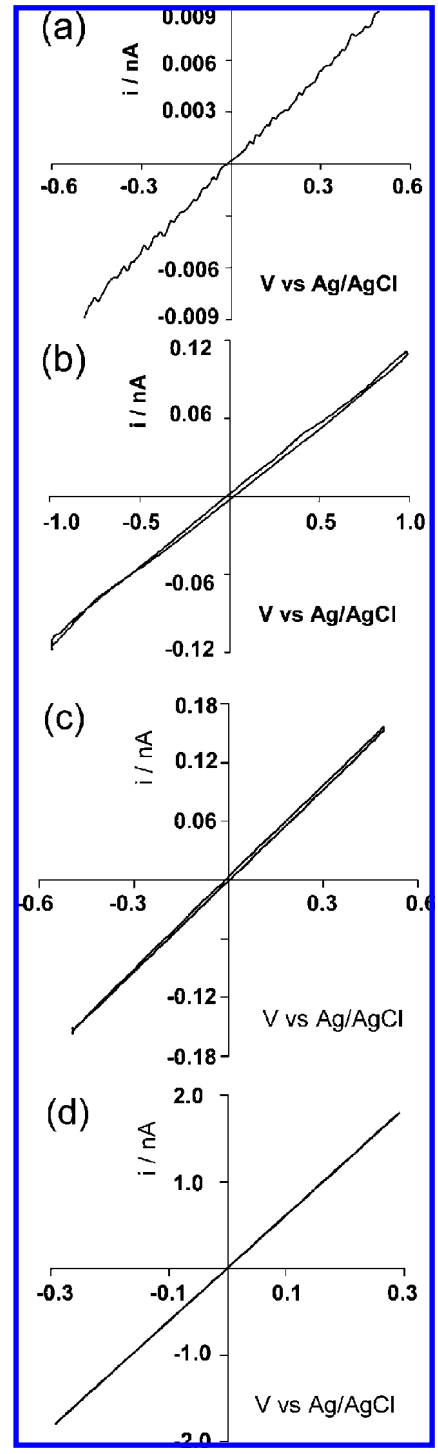

Figure 4. Current−voltage response of silica nanochannels in a 1.0 M KCl solution containing 10 mM sodium phosphate buffer and 0.1% Triton X-100. The geometry of the channels are (a) $d = 9.2$ nm, $l = 42$ μm; (b) $d = 24$ nm, $l = 40$ μm; (c) $d = 45$ nm, $l = 50$ μm; (d) $d = 93$ nm, $l = 12$ μm.

phosphate buffer (pH = 7.4) containing 1 M KCl. Ohmic response has been obtained for all of the nanochannels measured in Figure 4 due to their cylindrical geometry. The diameters of the channels are calculated to be 9.2, 24, 45, and 93 nm, respectively, based on the ionic resistance measured in Figure 4a−d.

Sensing of Polystyrene Nanoparticles. A 10 mM sodium phosphate buffer (pH = 7.4) containing 1.0 M KCl and 0.1% Triton X-100 is added to both inside and outside of the micropipet. Figure 5a−c shows the current−time response of a 6 μm long, 130 nm silica nanochannel in a 1.0 M KCl solution containing 10 mM sodium phosphate buffer (pH = 7.4) and 0.1% Triton X-100 before (Figure 5a) and after (Figure 5, parts b and c) the addition of 4.7 nM PS nanoparticles (40 nm in diameter). One can see from the comparison of parts a and b of Figure 5 that the translocation of nanoparticles is easily detected as individual current pulses in the current−time response. Due to the carboxylic groups on the surface, the nanoparticles are negatively charged at pH = 7.4. Thus, the translocation through the nanochannel should be driven mainly by electrophoretic force, as shown in Figure 5b. The magnitude of the current change and the time duration for the translocation could depend on a number of experimental factors (e.g., electrolyte concentration, electrical field) and properties of the nanochannel (e.g., the size of the inner nanochannel and its

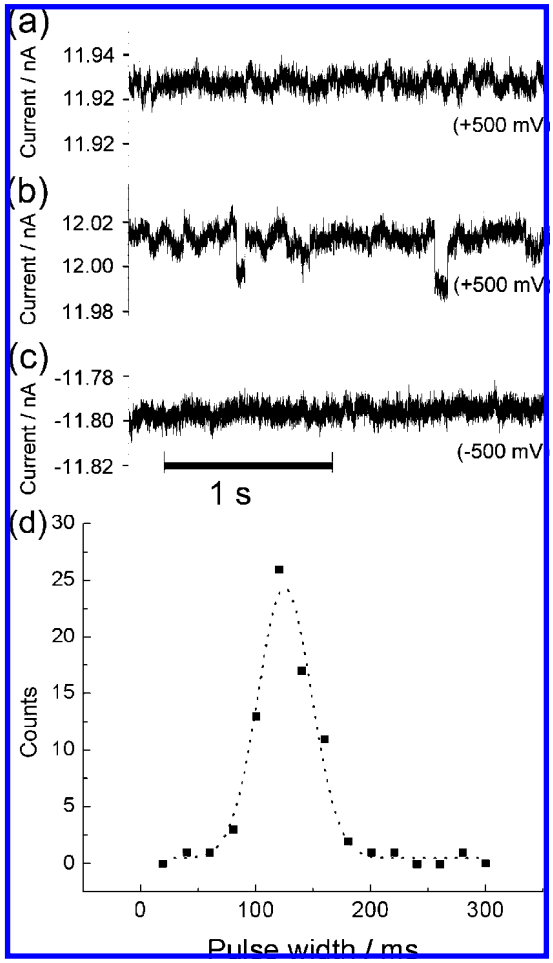

Figure 5. Current−time response of a 6 μm long 130 nm silica nanochannel in a 10 mM sodium phosphate buffer containing 1.0 M KCl and 0.1% (w/v) Triton X-100 without (a) and with (b and c) 4.7 nM polystyrene (PS) nanoparticles (40 nm). (d) A plot of the distribution of the transient time in panel b from a 6 min recording.

length, surface charges) and nanoparticles (e.g., the size and the number of surface charges).[8] Due to the relatively large length of the nanochannel, the magnitude of the current pulse is relatively small in our case, only 3 or 4 times larger than the noise level. However, this could be improved by shortening the length of the nanochannel and thus minimizing the volume of the inner capillary.[8]

A plot of the distribution of the transit time has been given in Figure 5d. As one can see, the distribution is wide and the mean pulse width is ~125 ms, which is much longer than what has been seen in the carbon nanochannel reported by the Crooks group.[8] There are a number of possible reasons leading to this large time duration. First, the channel length in our case is ~6 μm, which is almost an order of magnitude larger than the length of the carbon channel (~900 nm). Second, the walls on the silica channels are negatively charged, which could cause a significant flow of solvent in the opposite direction of the particle translocation due to electroosmosis (PS particles in this case are negatively charged). Third, due to the nature of the nanochannel, there could be a stronger interaction between the nanoparticles and the walls.

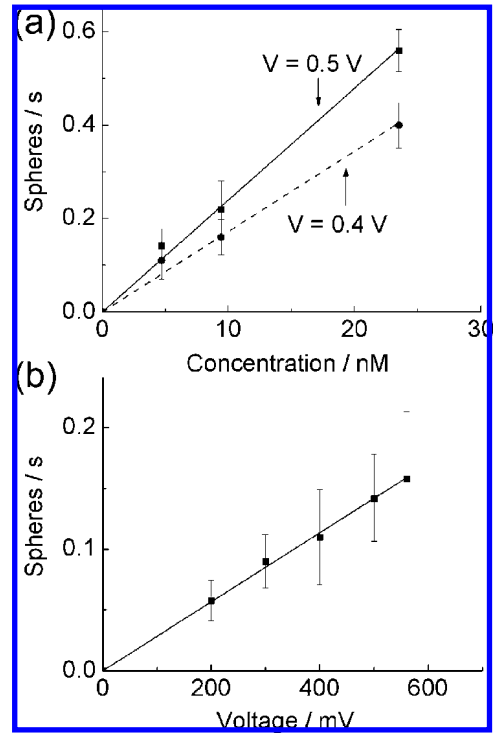

Figure 6. (a) Frequency of detection of polystyrene (PS) nanoparticles using a 130 nm silica nanochannel as a function of the concentration at two different voltages, solid = 0.5 V and dashed = 0.4 V, respectively. (b) The frequency of detection as a function of the voltage bias in a 4.7 nM solution.

Figure 6 shows the concentration dependence (Figure 6a) and the voltage dependence (Figure 6, parts a and b) in the translocation of nanoparticles. The number of particles was counted for at least 6 min for each experimental condition. As one can see from Figure 6a, the translocation rate is proportional to the concentration of the nanoparticles in the range of 0−25 nM at both 400 and 500 mV bias voltages. The frequencies of detection at the higher bias voltage are higher than at the lower voltage for all the concentrations, which also indicates the translocation is mainly driven by electrophoretic force. The similar trend has been shown in Figure 6b, where the frequency of detection is plotted as a function of the bias voltage for six different voltages in a solution containing 4.7 nM nanoparticles. As shown in Figure 6b, a linear relationship has been clearly shown between the frequency of detection and the applied bias voltage.

Translocation of DNA through Silica Nanochannels. The above experimental results show that the electrophoretic force is the main driving force for PS nanoparticles through a 130 nm channel. However, this is unlikely to be the case for the translocation of double-stranded λ-DNAs through a 9.0 nm nanochannel, as is shown in our following experiments. Figure 7a displays the current−time trace of a 35 μm long silica channel with a 9.0 nm diameter in a 3 M KCl solution at −600 mV bias voltage. Figure 7b shows the current−time response in the same solution after the addition of 6 μg/mL λ-DNA. An ~20% drop in the baseline current is immediately noticeable from part a to part b of Figure 7. We are not exactly sure as to why the current drops when DNAs are added. However, one possible reason could be that the DNA molecules are constantly interacting with the nanochannel orifice before they can find the right configuration

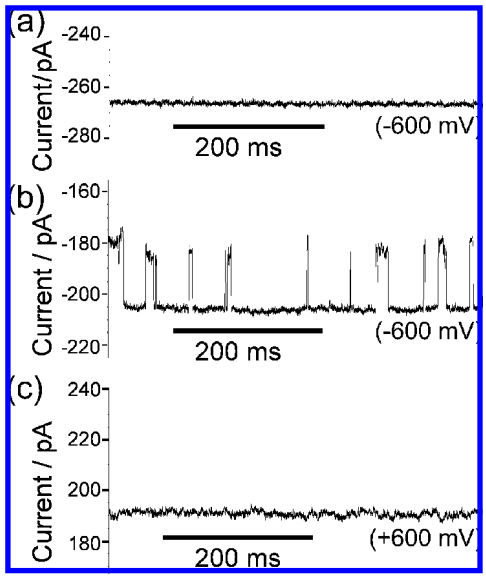

Figure 7. Current−time traces of a 9.0 nm channel in a 3 M KCl solution before (a) and after (b and c) adding 6 μg/mL λ-DNA. The bias voltage is −600 mV for panels a and b and +600 mV for panel c.

to actually fit into the nanochannel. This interaction may cause significant increase in the ionic resistance. Individual current pulses are detected in the response, indicating translocation of individual DNA molecules. However, when the bias voltage is switched from −600 to +600 mV, as shown in Figure 7c, no pulse signals are detected. *This is an interesting result because DNA translocation happens only when a negative bias voltage is applied, which means that the translocation of DNA is in the direction of the electric field.* This result suggests that the translocation of λ-DNA, in our case, is caused by electroosmotic flow instead of the electrophoretic force as seen in many other cases where nanochannels with smaller aspect ratio (l/d) are used.[33,34] The electroosmosis-driven DNA translocation might be due to a combination of the small size (and thus the large aspect ratio, ~3890) and the negative surface charges of the silica nanochannel and the relatively small electrical field (therefore, a minor electrophoretic driving force).

The translocation of DNA can be contributed from the following four different mechanisms: pressure-driven flow, electrophoresis, electroosmosis, and diffusion.[8] In our case, only electrophoresis and electroosmosis need to be considered because of the following reasons: first, the pressure-driven flow can be neglected since no pressure difference is applied at different sides of the nanochannel; second, the contribution from the diffusion is small because of the low concentration and a large confinement energy of DNA inside a 1D nanochannel. For the 9.0 nm channel at 0.6 V, the electrical field inside the nanochannel is approximately 1.7×10^4 V/m, which is close in magnitude to the electrical field in a typically capillary electrophoresis (CE)-type experiment (e.g., $E = 2.0 \times 10^4$ V/m when a 10 kV voltage is applied across a 50 cm long capillary). Therefore, a relatively large electroosmotic flow could be generated at this condition. In fact, it could be larger than that in the typical CE separation channel due to more overlapping of the electrical double layer. It has been suggested that extremely high static pressure can be generated across a nanometer-scale channel due to high electroosmosis in aqueous solutions. For example, Takamura et al. have reported the generation of up to 5000 Pa pressure across a 120 nm channel (length = 100 μm) in a phosphate buffer.[35] In addition, they have observed that smaller channels result in larger static pressures. Therefore, the static pressure across the nanochannel of ~10 nm could be much larger than what they measured across the 120 nm channel. Thus, the electroosmosis can be strong enough to overcome the electrophoretic force and push the DNA molecule through the nanochannel.

The electrophoretic force would drive the DNA molecules in the opposite direction. However, it could be less important as compared to the electroosmotic flow. In the traditional nanopore-type experiments, the thickness of the membrane is usually on the order of 10−100 nm. Therefore, the electrical field inside the nanopore could be as high as 10^7 V/m when a 100 mV voltage is applied across the membrane, which is almost 3 orders of magnitude larger than the electrical field in the nanochannel. Thus, the electrophoretic driving force can be neglected when a strong electroosmosis exists. Since the electroosmosis effect decreases as the channel is larger, one would expect to see electrophoretic-driven DNA transport when a larger silica channel is utilized. In fact, when another nanochannel (with a larger diameter, d = 75 nm, and a smaller length, l = 15 μm) is used for the same experiment, DNA translocation is observed to be electrophoretically driven. Figure 8 displays a current−time response at +400 mV of a 75 nm channel in a 1 M KCl solution in the absence (Figure 8a) and presence (Figure 8b) of 3 μg/mL λ-DNA. Figure 8c shows the current−time response when the voltage is switched from +400 to −400 mV. Current pulses are only seen when a positive bias voltage is applied, which indicates that DNA molecules are driven in the opposite direction of the electrical field. Because the size of the nanochannel is almost an order magnitude larger in this case, we anticipate less overlap from the electrical double layer. Therefore, an electrophoresis-driven flow could dominate the translocation of DNA. Chou's group recently reported the translocation of fluorescently labeled genomic-length DNAs through an ultralong 50 nm square channel using electrophoresis.[24] They also reported that they were unable to electrophoretically drive DNA molecules through 20 nm wide channels. However, they explained the difference to the large entropic change and the effects of the surface charges.

The frequency of DNA translocations has been found to be dependent on the applied voltage. No translocation of DNA has been observed at voltages below ~200 mV, which might indicate the presence of a minimum driving force for the DNA molecules to uncoil as they are driven through the nanochannel. It increases when the voltage is increased. Figure 9 displays the current−time responses of DNA translocation at different bias voltages for the 9.0 nm channel in a 3 M KCl solution containing 6 μg/mL of DNA. As shown in Figure 9a, there are no current pulses present in the current−time response when a −200 mV bias is applied. Figure

(33) Wanunu, M.; Sutin, J.; McNally, B.; Chow, A.; Meller, A. *Biophys. J.* **2008**, *95*, 4716–4725.
(34) Fan, R.; Karnik, R.; Yue, M.; Li, D.; Majumdar, A.; Yang, P. *Nano Lett.* **2005**, *5*, 1633–1637.
(35) Takamura, Y.; Onoda, H.; Inokuchi, H.; Adachi, S.; Oki, A.; Horiike, Y. *Electrophoresis* **2003**, *24*, 185–192.

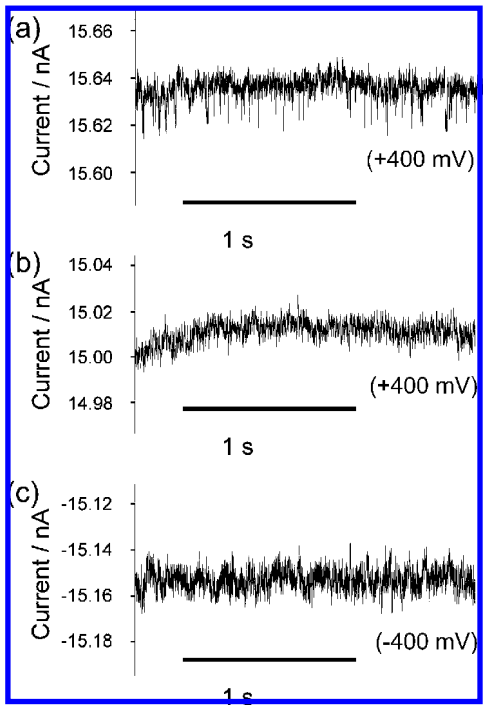

Figure 8. Current−time traces of a 75 nm nanochannel in 1 M KCl solution before (a) and after (b and c) adding 3 μg/mL λ-DNA. The bias voltage is +400 mV for panels a and b and −400 mV for panel c.

9b displays the current−time response when the bias is increased to −300 mV. Current pulses start to appear on the current−time response at this bias voltage. However, the frequency of DNA translocation is relatively low as compared to the higher voltages. When the bias voltage is increased to −400 mV, as shown in Figure 9c, more frequent current pulses are observed. A comparison of the results from parts b and c of Figure 9 also reveals that the pulses at higher voltages are shorter in length than those at lower voltages, reflecting the differences in DNA translocation speed inside the nanochannel.

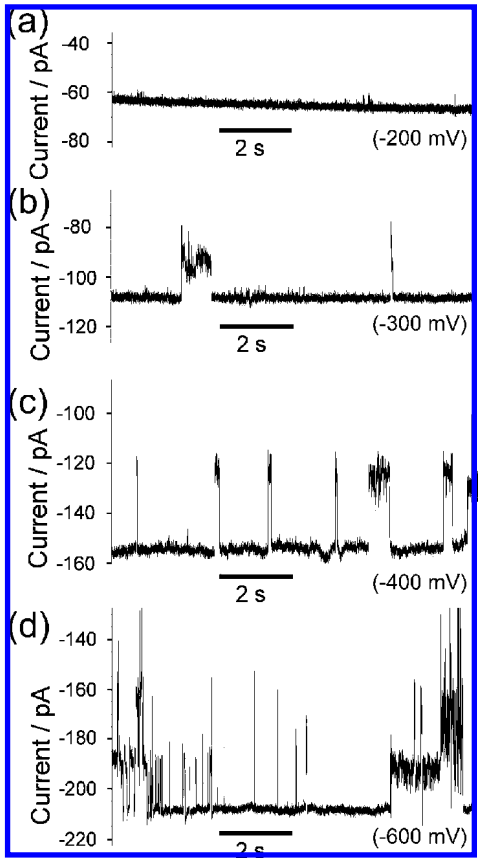

Figure 9. Current−time traces of a 9.0 nm channel in a 3 M KCl solution containing 6 μg/mL λ-DNA at different bias voltages: −200 (a), −300 (b), −400 (c), and −600 mV (d).

Another interesting aspect of the response is that some current pulses are doubled or even tripled in magnitude at higher voltages. In other words, a narrow pulse is formed on top of another wider pulse. A closer examination of parts c and d of Figure 9 reveals that there are more of these higher pulses at −600 mV than at −400 mV. In fact, there are no such higher pulses observed at voltages lower than −400 mV. More importantly, the magnitude of these higher pulses is roughly 2 or 3 times the lower signals. Another distinct characteristic is that the higher pulses are usually seen on top of a lower pulse. The length of these higher pulses is also shorter than the lower ones. A possible explanation for the appearance of these higher pulses is that multiple DNA molecules are present simultaneously inside the nanochannel at higher voltages. The equilibrium radius for λ-DNA is estimated to be 0.73 μm,[36] which is 2 orders of magnitude larger than the size of the smaller nanochannel. This indicates that the DNAs are fully stretched when they are inside the 1D channel. The end-to-end length of the electrically stretched λ-DNAs is in the range of 6−16 μm depending on the experimental conditions, as estimated or measured by a number of different methods.[9,37] Therefore, it is possible that up to three or four DNA molecules can be accommodated simultaneously inside the same nanochannel ($l = 35\ \mu$m). Further experiments are obviously required to study more details in DNA translocations through nanochannels of these dimensions. This type of experiment is currently ongoing in our laboratory and will be reported in future publications.

CONCLUSION

We have presented a novel method of preparing nanometer-scale silica channels of cylindrical shape. Nanochannels from 5 to 100 nm in diameter can be readily made from mechanically pulled silica capillary preforms. These nanochannels are easy to make, robust, well-defined in geometry, and could be easily functionalized using silane chemistry. Optical microscopy, SEM, and resistance measurements have been utilized to characterize the geometry of these silica nanochannels. Polystyrene nanoparticles of 40 nm in diameter have been detected using these silica nanochannel sensors. The frequency of detection has been found to be linearly dependent on both the concentration of the nanoparticle and the applied voltage, indicating electrophoresis-driven translocation of the nanoparticles. Genomic-length double-stranded DNA molecules have been used to demonstrate the application of our silica nanochannels in the study of molecular transport through nanofluidic channels. The results show that the translocation of DNA molecules is possibly driven by electroos-

(36) Stein, D.; van der Heyden, F. H. J.; Koopmans, W. J. A.; Dekker, C. *Proc. Natl. Acad. Sci. U.S.A.* **2006**, *103*, 15853–15858.
(37) Sanger, F.; Coulson, A. R.; Hong, G. F.; Hill, D. F.; Petersen, G. B. *J. Mol. Biol.* **1982**, *162*, 729–773.

motic flow in a 9.0 nm channel, whereas it is driven by electrophoretic force in a 75 nm channel at the similar conditions.

ACKNOWLEDGMENT

The authors thank the University of Washington for the financial support. Part of this work was conducted at the University of Washington NanoTech User Facility, a member of the NSF National Nanotechnology Infrastructure Network (NNIN).

SUPPORTING INFORMATION AVAILABLE

Schematic of the process to make silica nanochannels and pulse signals showing possible detections of two nanospheres within one channel. This material is available free of charge via the Internet at http://pubs.acs.org.

Received for review April 28, 2009. Accepted May 22, 2009.

AC9009148